UNIVERSITY OF
BIRMINGHAM

Year 3 Laboratory:
Interactions of Neutrons with Matter

School of Physics and Astronomy
University of Birmingham

Josh Wainwright
UID:1079596

Demonstrators: Dr Peter Jones, Dr Garry Tungate,
Dr Carl Wheldon, Dr Neil Curtis
Date: December 2012

Contents

1 Introduction

This experiment involves examining the interactions of neutrons with matter through two experiments using two different detectors. The first detector, a sodium iodide scintillation detector will be used to measure the binding energy of the neutron, and secondly, using a boron-trifluoride counter, measure the moderating properties of water on fast neutrons as a function of radius from a central source.

2 Neutron Binding Energy

2.1 Sodium Iodide Detector

The sodium iodide detector is a scintillation detector that uses a NaI crystal doped with thallium to create scintillation photons when a gamma ray photon hits the crystal. The thallium is added as an activator to provide extra available energy levels for the photons in the crystal to occupy. In the pure state, the NaI has a large forbidden band gap between the conduction and valence bands, shown in figure 1. The activator reduces this gap so that an emitted photon is in the range that the photomultiplier tube is sensitive to, typically visible.

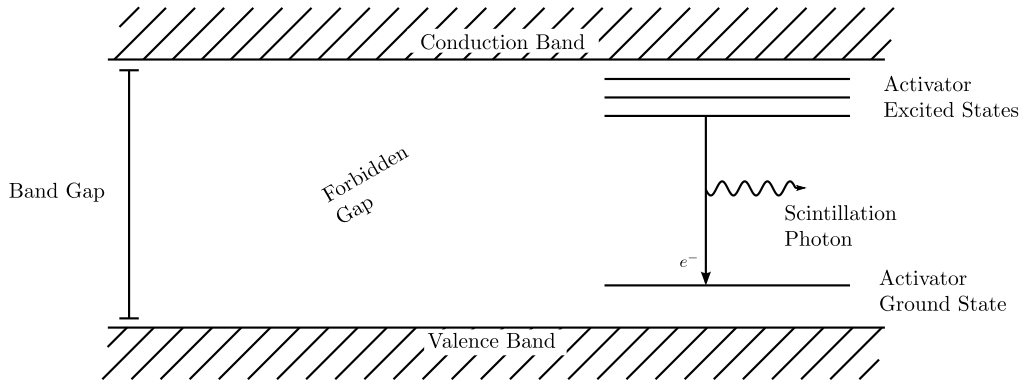

Figure 1: *The element thallium is added to the pure crystal of sodium iodide to provide extra energy levels for the electrons, which sit inside the forbidden gap of the crystal latice structure. These allow a photon of a useful wavelength to be emitted when electron decays to a lower energy.*

When a gamma photon enters the detector it ionises a molecule of NaI creating excited states in the crystal that then decay via visible photons. The number of photons that are produced is proportional to the energy of the incident photon, as the energy of the gamma ray increases, more scintillation photons are produced. Thus, the energy of the original can be found be counting the number of photons produced.

These scintillation photons are used to create electrons which are more easily counted. At the photo-cathode, the photons release electrons via the photoelectric effect. The electrons are then passed through the photomultiplier tube which increases the number of photons linearly by accelerating them through a high potential difference so they can knock more electrons out from the dynodes (see figure 2). This results in a stream of electrons that can be measured, and which is proportional to the original energy of the photon via the number of scintillation photons, the number of electrons and the multiplication factor of the increase of electrons from the PM tube. Since each of these steps is a linear relationship, a calibration setting can be taken using known results, and a simple linear equation relating the reading taken to the energy of the photon found.

The detector requires a high voltage which is placed across the dynodes and the anode to accelerate the electrons once they have entered the PM tube. Using this method of acceleration

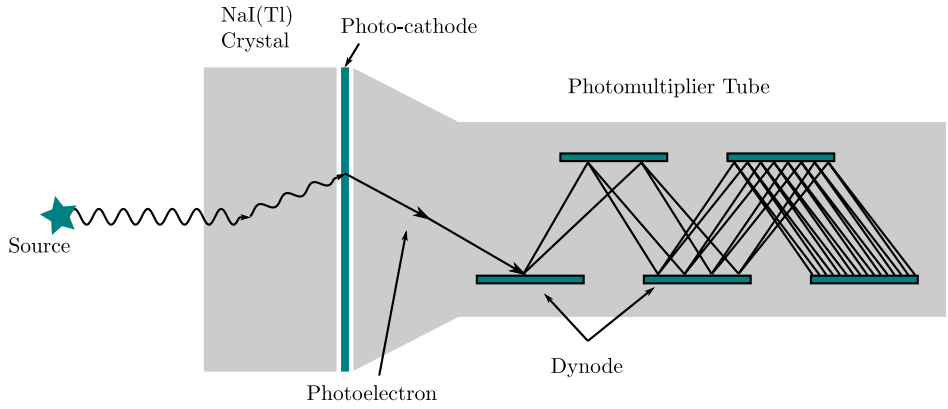

Figure 2: *The sodium iodide detector is a commonly used gamma ray detector that uses the relationship between the energy of a photon and the ionisation power that it has to measure its energy via a calibration equation.*

and re-acceleration, the photomultiplier tube is able to increase the number of electrons by a factor of roughly 10^5 depending on the voltage bias.

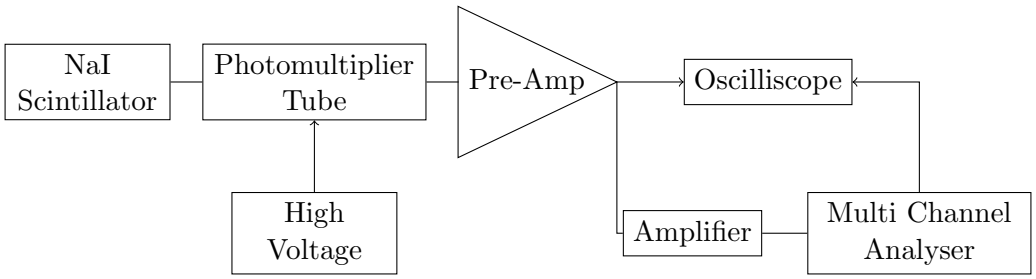

2.2 Calibration

Before any data can be read from the spectra taken from the detector, the data has to be calibrated. To do this, a set of known samples with well defined peaks is used to get a relation between the channel number of an observed peak and its energy. Once this is done, a relation can be found that relates the channel number to energy for use on later measurements.

The elements that were used included cobalt, barium, caesium, europium and americium. Each of these elements were available to measure, and each has recorded and accepted peaks that are at well defined positions. The data was taken from the National Nuclear Data Centre (NNDC). The table below, table 1, shows the data that we collected from these sources. The channel number refers to the position in the spectrum that the peak was observed and the expected peak is the energy of the peak that the respective peak is estimated to correspond to.

From these, the graph in figure 3 can be drawn which shows the relation that can be used as a calibration between energy and channel number. The exact value of this relation, intercept and gradient, are subject to change since the calibration is retaken at the start of each session to account for changes in the experimental set-up and the radioactivity of the source which will decrease with time.

An example of the spectra from the sources is shown in figure 4. This shows the spectrum of ^{60}Co which has been fitted with the Gaussian peaks to find the position and FWHM using the "root" package.

This line has the equation,

$$E = 3.63 \times x - 18.31 \tag{2.1}$$

Element		Channel Number	Expected Peak Energy (keV)
Cobolt	^{60}Co	369.4	1332.0
		324.9	1173.0
Barium	^{133}Ba	102.9	356.0
		86.08	302.9
Caesium	^{137}Cs	188.4	661.7
Europium	^{152}Eu	99.84	344.3
		222.0	778.9
		274.9	964.1
		311.0	1121/1086
		394.1	1408.0

Table 1: *Several elements were used to measure a calibration relation that links the observed channel number to the energy.*

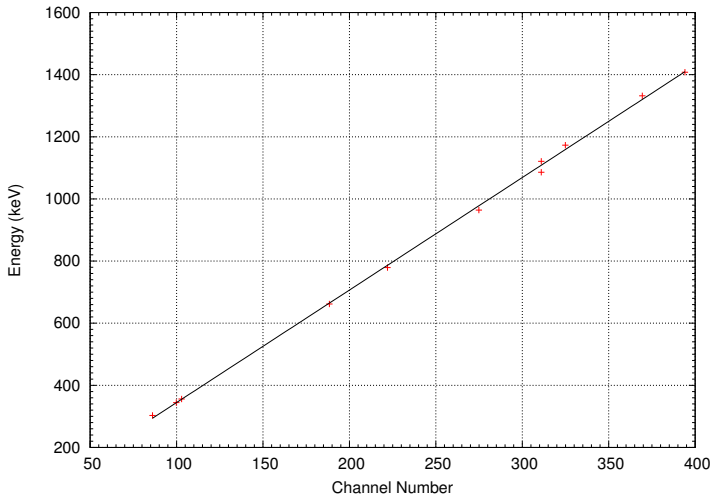

Figure 3: *The sodium iodide detector provides a channel number readout that is directly proportional to the energy of the corresponding reaction event. Thus, using known data points, a relation between channel number and energy can be found.*

This equation, equation 2.1, shall be used as the calibration equation for the sodium iodide experiment. The calibration was re-taken at the start of each session using the NaI detector, so this value represents the session where the actual experimental results were taken for the main section of finding the deuteron binding energy.

2.3 Energy Resolution

Scintillation detectors, such as the NaI detector in use here, have a relatively poor energy resolution. Statistical broadening of the peaks is usually the dominant form of broadening. When a reaction takes place, and so energy is deposited, in the scintillator crystal, the efficiency can be as low as around 10%. This means that a far smaller amount of energy is actually transferred to the crystal than the energy of the incoming particle.

When the reaction takes place in the crystal, a number of photons, proportional to the energy deposited, are produced. But some of them are lost before they can reach the photomultiplier tube further reducing the measured number of photons. This also means that there is a minimum in the number of photons just before the photomultiplier tube. Since the number of arriving photons will be subject to statistical fluctuations, the standard deviation in the photons reaching

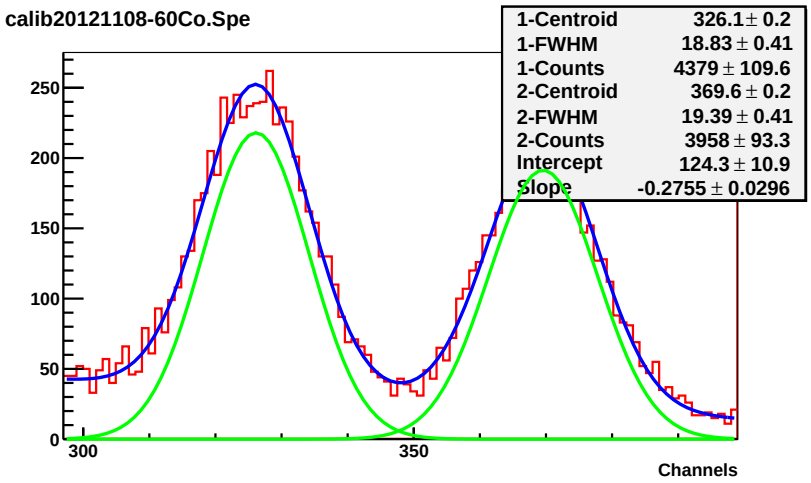

Figure 4: *An example of the peak for the radioactive element cobalt-60. These two peaks are well defined and have well known values. This means that they are good for using as calibration points for the detector.*

the PM tube is given by equation 2.2,

$$\text{Standard Deviation, } \sigma = \sqrt{\text{Number of photons reaching the PM tube}} \tag{2.2}$$

Since this is proportional to the energy of the original photon that caused the reaction, it can be shown that

$$R = \frac{\text{FWHM}}{H_0} \tag{2.3}$$

$$= k\frac{\sqrt{E}}{E} = \frac{k}{\sqrt{E}} \tag{2.4}$$

Where FWHM is the full width at half maximum of any given peak, H_0 is the height of the peak and k is a constant of proportionality. This means that the resolution can be easily observed by plotting a graph of $\log k$ against $\log E$, which should give a slope of $-\frac{1}{2}$ in an ideal case.

The resolution of the NaI detector is use was measured using the method described above.

2.4 Neutron Binding Energy

The first full experiment that was attempted was measuring the binding energy of neutrons by observing the γ-ray emitted when the neutrons are captured by protons in the water surrounding a neutron source via reaction 2.5,

$$^1_1\text{p} + ^0_1\text{n} \rightarrow ^1_2\text{d} + \gamma \tag{2.5}$$

The exact energy would be found from the peak from this photon observed in the spectrum.

In order to observe the spectrum as clearly as possible, the experiment was run overnight collecting data for approximately 25 hours. This would give us a much clear spectrum and so lower errors on the final data. The spectrum that was recorded is shown in figure 5, along with a description of each of the major peaks that are visible. This plot is shown on a single $\log y$ axis so that the peaks are more easily discernible.

The major peaks, from figure 5 are as follows:

1. 511 keV peak from the electron rest mass.

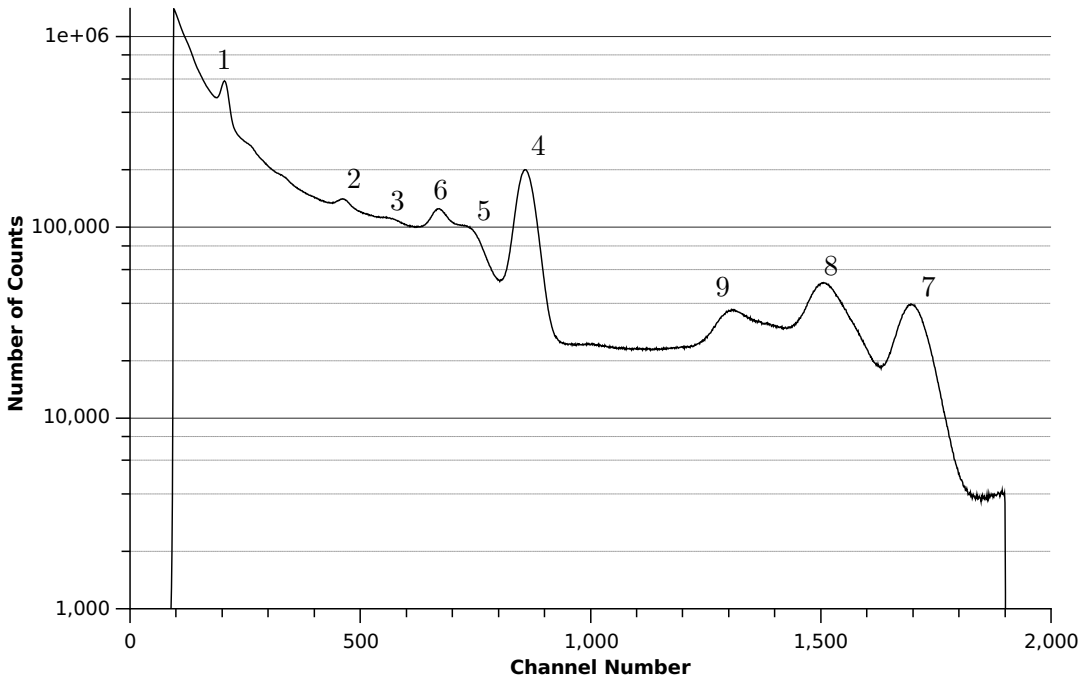

Figure 5: *The spectrum from the neutron tank observing a radioactive neutron emitter for a prolonged period of time.*

2. Unknown.
3. Double escape peak?.
4. **Neutron binding energy**.
5. Unknown
6. Single escape peak from the neutron binding energy.
   Double escape peak from the neutron binding energy.
7. Reaction peak from either oxygen ($^{8}O_2$) or carbon (^{12}C) from the water in the tank. Further investigation would be needed to determine the exact cause of this peak since it is so weak in comparison to the others.
8. Escape peak from the carbon/oxygen peak
9. Double escape peak from the carbon/oxygen peak

2.4.1 Escape Peaks

The peaks that are labelled as "escape peaks" from the previous graph, figure 5, are due to the phenomena called pair production. Pair production occurs if the incident energy is above 1022 keV, i.e. twice the rest mass of the electron, and results in the production of two 511 keV annihilation gamma rays. If one of these gamma rays escapes the detector while the other is completely absorbed, 511 keV will be lost from the detector. This results in a separate peak in the spectrum representing the original energy minus 511 keV. This is called a single escape peak. If both annihilation gamma-rays escape the detector a double escape peak is formed with an energy of the expected energy minus 2× 511 keV, or 1022 keV.

Escape peaks can seen whenever there are events with energies greater than the 1022 keV limit. They are generally slightly lower in height than the main peak and are always at the same distance from the main peak.

2.4.2 Background Radiation

This experiment was carried out using a sample of americium-beryllium (AmBe) and as such, the peaks seen in the resulting spectrum should be well known and well defined. Instead, there are a number of peaks that cannot, at the present time, be accounted for. There are several explanations to explain these peaks.

1. The first is the method of creating the samples in use. The samples were made by bombarding the metals using a synchrotron particle accelerator. This has the effect of possibly creating an impure sample so that there are other elements that are decaying producing their own spectrum that is adding the the expected one.
2. Another possibility is that the other radiation sources that are stored nearby introduced extra peaks from their own radioactive decays.

2.5 Experimental Results

The calibration data that was taken gave a channel number-energy relation of

$$E = 3.63 \times C - 18.31 \tag{2.6}$$

where E is the actual energy and C is the observed channel number. Using this equation, peak number 5 from the above spectrum, figure 5, is found to lie at an energy of 2.244 ± 0.048 MeV. The data taken from the spectrum is shown in table 2. This table shows the channel number of each of the peaks labelled above, the error on this position, the energy and corresponding error for the peak and the differences between some of the adjacent peaks. This last column is used to verify escape peaks which are always at 511 keV below the main peak.

Channel №	Error on Channel №	Energy	Error on Energy	Difference
181.20	0.07	496	31	
232.45	0.02	651	32	
403.33	0.15	1170	36	
458.6	0.18	1338	38	
617.3	0.56	1820	43	482
757.2	0.08	2244	48	425
1168.5	13.0	3492	66	1248
1335.4	0.50	3999	73	507
1496.6	0.28	4488	81	489

Table 2: *Values for the channel numbers and corresponding energies of the peaks from the spectrum of the BeAm sample in the water tank.*

The values for the channel numbers, along with the corresponding errors, in table 2, were taken from the results of the peak fitting algorithm, "Buffit", provided as an extension to be used with the "root" interpreter framework. An example of this peak fitting is shown below in figure 6.

The value for the errors on the energies calculated here are given equation 2.7.

$$(\sigma E)^2 = (\sigma Ch \times m)^2 + (\sigma m \times Ch)^2 + (\sigma c)^2 \tag{2.7}$$

where

σE is the error on the energy

Ch is the channel number from the detector

m is the gradient of the line fit of the data

c is the intercept of the line fit.

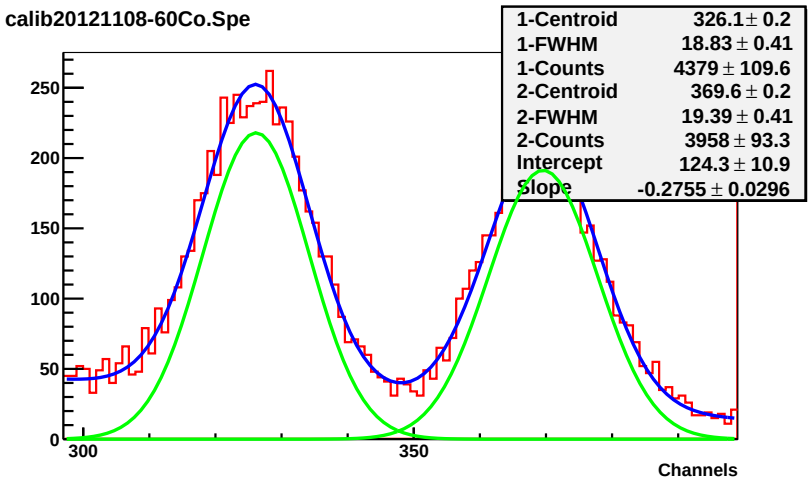

Figure 6: *An example of the peak for the radioactive element cobalt-60. These two peaks are well defined and have well known values. This means that they are good for using as calibration points for the detector.*

2.6 Analysis of Experimental Results

The binding energy of the deuteron can be found theoretically from the mass difference between the deuteron and its individual components, as follows.

$$ {}^{1}_{0}\mathrm{n} + {}^{1}_{1}\mathrm{p} \rightarrow {}^{2}_{1}\mathrm{d} + \gamma \tag{2.8} $$

The mass excess of each of these is as follows

$$ \Delta^{1}\mathrm{p} = 7.2889\mathrm{MeV} $$
$$ \Delta^{1}\mathrm{n} = 8.0713\mathrm{MeV} $$
$$ \Delta^{2}\mathrm{d} = 13.1357\mathrm{MeV} $$

The binding energy is thus

$$ 7.2889 + 8.0713 + 13.1357 = 2.2245\mathrm{MeV} \tag{2.9} $$

We can also find the difference between the binding energy of ^{16}O and ^{17}O from

$$ {}^{16}_{8}\mathrm{O} + {}^{1}_{0}\mathrm{n} \rightarrow {}^{17}_{8}\mathrm{O} + \gamma \tag{2.10} $$

For this reaction, the mass excesses are

$$ \Delta^{16}\mathrm{O} = -4.7370\mathrm{MeV} $$
$$ \Delta^{17}\mathrm{O} = -0.8087\mathrm{MeV} $$
$$ \Delta^{1}\mathrm{n} = 8.0713\mathrm{MeV} $$

This confirms that the peak labelled number 4 is indeed in the correct energy location to be the binding energy of the neutron, and provides good evidence that the final unknown peak, peak number 7, could be from the oxygen in the water in the tank.

3 Neutron Attenuation In Water

3.1 Boron Tri-Flouride Detector

The BF_3 detector is a proportional counter. It contains boron trifluoride gas at 0.5 to 1 atmospheres which acts as both a target for slow neutron conversion into secondary particles, as well as a proportional gas. A large potential difference is applied across the gas. The cathode which is held at ground is the outer tube of the detector and is generally made from aluminium since this has a low neutron absorption cross section so should not influence any readings made by the detector. The anode, at high voltage, is a single wire that passes through the centre of the detector, see figure 7. When a neutron is incident in the reactor, one of the reaction below takes place.

$$^{10}_{5}\mathrm{B} + ^{1}_{0}\mathrm{n} \rightarrow ^{7}_{3}\mathrm{Li} + ^{4}_{2}\alpha \tag{3.1}$$

$$^{10}_{5}\mathrm{B} + ^{1}_{0}\mathrm{n} \rightarrow ^{7}_{3}\mathrm{Li}^{*} + ^{4}_{2}\alpha \tag{3.2}$$

The products of these two equations differ only by the energy of the lithium which, in some cases, is left in an excited metastable state with a slightly different energy. The relative probabilities of each reaction is 96% for equation 3.1 and 4% for equation 3.2. The resulting ions that are created are attracted to the poles of the detector and so provide a voltage through it. This provides a signal which is sent to the processing computer. It should be noted that this detector cannot give any information of the energy of the neutron since the formation of the ions is independent of energy over a certain level. Instead, this detector is used simply as a counter to obtain a value for the number of neutrons hitting it in a specified time period.

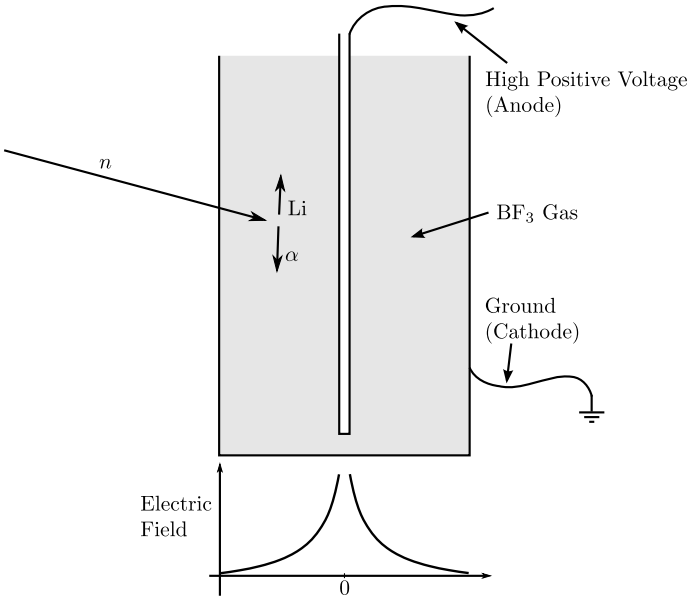

Figure 7: *The BF_4 detector uses a high charge to create a flow of ions to measure the incoming neutron. It cannot measure the energy, but simply gives a count for the number of neutrons incident in the detector. The anode and cathode create a large electric field inside the detector that creates the flow of charge used to count the incoming particles.*

When the reaction happens, the products, $^{7}_{3}Li$ and $^{4}_{2}\alpha$, are ejected through the BF_3 gas at a high velocity and can go on to cause further reactions in the gas as these ions deposit their kinetic energy. The electric field close to the wire increases quickly ($E \propto \frac{1}{r^2}$) and so a Townsend avalanche forms near to the wire when a reaction occurs. This involves the electrons being accelerated greatly by the electric field which causes the gas to conduct through the avalanche. The avalanche terminates when all of the free electrons reach the anode. These electrons produce

the signal which is measured by the computer and used for analysis. Despite the several steps involved, if the detector is well designed, the number of electrons that is measured can be ensured to be proportional to the incident energy of the particles.

3.1.1 Wall Effect

The BF_3 detector shall be used for several purposes later, so it is worth discussing some of the features of the data that is produced by this detector. Figure 8 shows a typical spectrum from the BF_3 detector. This shows a main peak, a smaller, higher energy secondary peak and an example of the wall effect.

When a neutron is incident with one of the atoms in the gas in the reactor, one of the reactions equation 3.1 or 3.2 takes place. If the reactor was extremely large compared to the travel distance of the Li and α products, then a single peak from each of the reactions would be observed, along with some amount of background noise, giving a spectrum similar to the top graph in figure 8. The two peaks are from the reaction producing a ground state lithium atom or an excited lithium atom respectively.

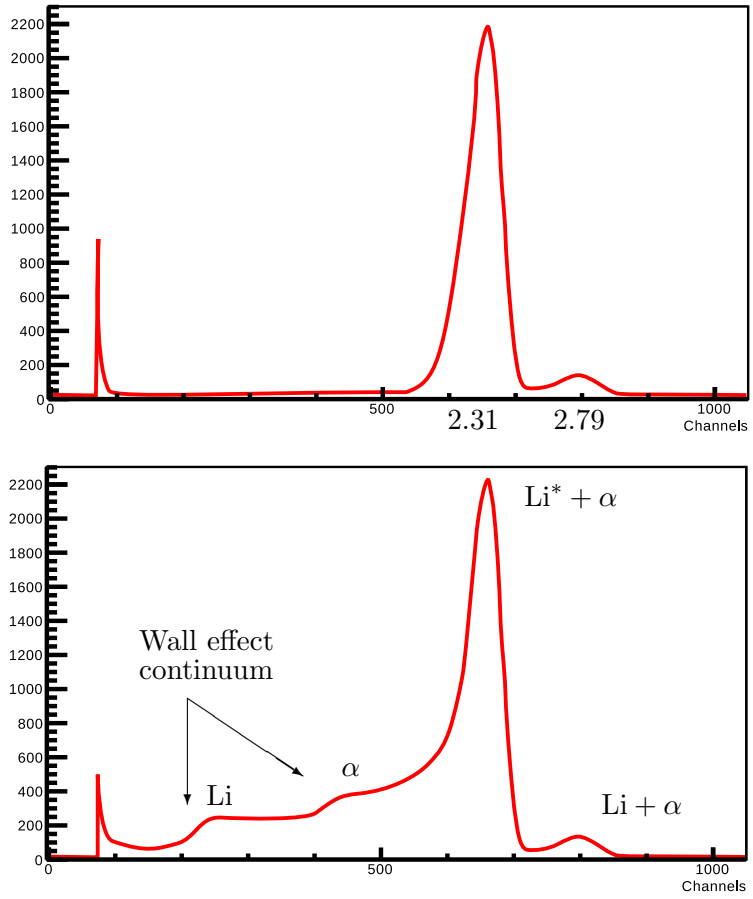

Figure 8: *An exemplar spectrum from the BF_3 detector showing the two peaks from each of the two reaction products, and the wall effect when one of the products from equation 3.1 escapes the detector.*

The two steps in the count number at lower channel numbers is known as the wall effect. These are due to the detector being finite, or small compared to the travel distance of the reaction products, and so there is a chance that one of the products from the reaction escapes from the detector. Due to the relative masses of the particles created, α and Li, the α particle takes most of the energy from the original neutron and so when it is lost from the detector, the recoded energy is lower.

Other features of the spectrum are the abrupt cut-off at the low channel numbers. This is to reduce the background counts that are present in this region from obscuring the rest of the data.

3.1.2 Boron Triflouride Detector Set-up

Since it is only a proportional counter, and so gives no information for the energy of the observed particles, there is no calibration to be done with the BF_3 detector. However, there is a certain degree of adjustment that can, and should, be made to the settings of the detector before proceeding with the data acquisition. The detector requires a high voltage of between 1.4 to 2.6 keV. This is the safe working range, but inside these limits, the voltage that gives the clearest results can be chosen. Figure 9 shows several graphs from the BF_3 detector using different voltages to ascertain which would be the most appropriate voltage to use.

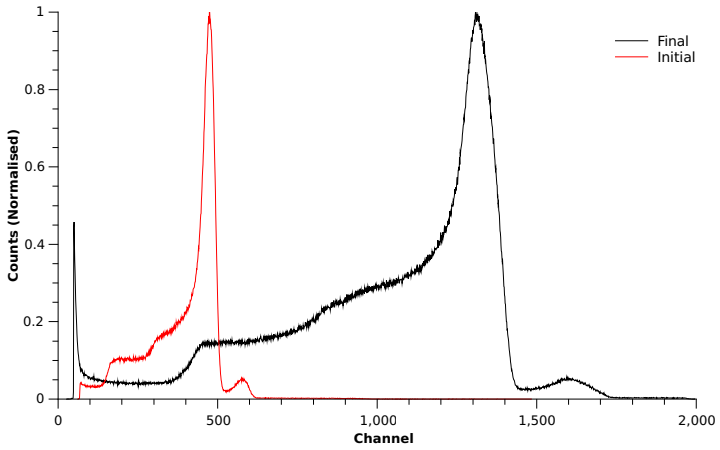

Figure 9: *The effect of adjusting the supplied voltage correctly. The initial readings, using the lower bound of the allowed voltage range does not make full use of the channel range and so any readings will be subject to higher errors. The final voltage level that was used takes full advantage of the channel width of the detector.*

3.2 Neutron Attenuation

In order to examine the attenuation effects of water to neutrons from the beryllium-americium source, the spectrum of neutrons will be measured with the BF_3 detector at a range of distances from the source, moving radially outward through the water. The readings shall be taken for precisely the same length of time using the built in timing function of the software used to record the readings. The count value from the data will be taken from the centre of the lower wall upwards, since everything below this point must be background radiation.

An estimate for the background radiation involved in the main section of the readings can also be made. By looking at the spectrum recorded from the detector, it can be seen that the background level just prior to the first wall, and so before any useful information from either reaction, and just after the second peak, can be joined by a straight line, representing a linear falloff of background across the channels. This is shown in figure 10. The count number represented by this triangle can be measured, and subtracted from the total count, which shall also be taken inside these limits. This should provide a reduced count number that has removed a significant proportion of the background that would have affected the result.

The total number of counts is a function provided by the software that is used, called Maestro. This allows us to easily record the number of counts for specific regions of the graph. Using this method, and initial trial recording was taken to work out an estimate for the percentage of the

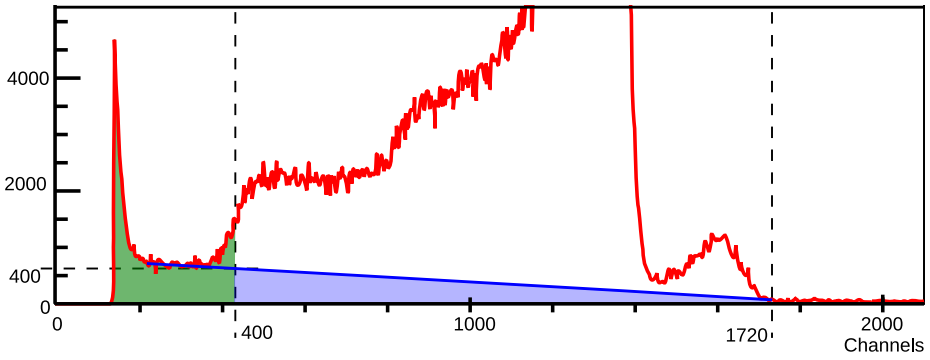

Figure 10: *An estimate of the background is made by assuming it falls linearly from the beggining of the channel numbers, which has to be error, to a point where it is known to be zero, after the second peak. The green shaded region is known to background since the second step represents the loss of both the lithium and the α particles.*

total counts were contributed by this background radiation. Equation 3.3 shows the calculation used to calculate the background,

$$(1729 - 400) \times 400 \times 0.5 = 264,000 \,\text{counts} \tag{3.3}$$

The total counts, including this noise, was 3.82×10^6, hence, the background represents roughly 6.9% of the total counts.

3.3 Experimental Results

3.4 Neutron Attenuation Theory

In order to model the situation, in a simplified way, the statistical one-group approach is used. It shall be assumed that all of the neutrons are thermalised, reduced in speed to similar to the surrounding particles, and an estimate for the diffusion length can be found. The diffusion length is the distance a thermal, or fast travelling neutron, takes to slow down. Once it has been thermalised, the neutron can be absorbed by matter, for example, an oxygen atom in the water surrounding the source. Thermalisation is the best method for reducing the speed of neutrons for many applications, since neutrons are not charged particles and so do not interact with electric or magnetic fields.

The Americium-Beryllium source that was used was assumed to be a point source, which is a good approximation compared with the distances that we are measuring, and so the emitting of neutrons from such a source is given by

$$\frac{\mathrm{d}n}{\mathrm{d}t} = -\Sigma_a \phi - \nabla \cdot \mathbf{J} \tag{3.4}$$

where n is the number of neutrons at time t, Σ_a is the absorption cross section of the water in the tank, ϕ is the neutron flux (number of neutrons travelling through a unit are in unit time) and the vector $\mathbf{J}$ is the diffusion flux from Fick's law shown in equation 3.5,

$$\mathbf{J} = -\mathbf{D}\nabla\phi \tag{3.5}$$

This means that the term from equation 3.4, $-\Sigma_a\phi$ is the loss of neutrons due to absorption, and the term $-\nabla \cdot \mathbf{J}$ is the divergence. Since the flux is simply the number passing a static point multiplied by their velocity, $\phi = nv$, equation 3.4 can be written as

$$\frac{1}{v}\frac{\mathrm{d}\phi}{\mathrm{d}t} = -\Sigma_a\phi + D\nabla^2\phi^2 \tag{3.6}$$

But in the steady state, $\frac{\mathrm{d}\phi}{\mathrm{d}t} = 0$, so

$$\Sigma_a \phi = D\nabla^2 \phi \tag{3.7}$$

The region of interest around the source, the water tank filled with water, has cylindrical symmetry but also, up to a radius of roughly 0.5 m has spherical symmetry. In this case, the neutron flux is independent of the angle measured at and so this equation can be simplified to to a single dimension.

$$\frac{1}{r^2}\frac{\mathrm{d}}{\mathrm{d}r^2}\left(r^2\frac{\mathrm{d}\phi_r}{\mathrm{d}r} - \frac{1}{L^2}\phi_r\right) = 0 \tag{3.8}$$

where the diffusion length, L, which is the distance travelled by an average neutron through the water, is given by

$$L = \sqrt{\frac{D}{\Sigma_a}}. \tag{3.9}$$

The solutions of the equation 3.8 have the form

$$\phi = A\frac{e^{-\frac{r}{L}}}{r} + B\frac{e^{\frac{r}{L}}}{r} \tag{3.10}$$

To simplify this equation, it is assumed that the coefficient, B, is zero, since otherwise the second term would tend to infinity as the radius increases, which is clearly un-physical. This leaves the following equation

$$\phi = A\frac{e^{-\frac{r}{L}}}{r} \tag{3.11}$$

$$r\phi \propto e^{-\frac{r}{L}} \tag{3.12}$$

Thus, when $\ln(r\phi)$ is plotted against r, the graph should have a gradient of $-\frac{1}{L}$